ADVANCES IN ATMOSPHERIC SCIENCES, VOL. 29, NO. 3, 2012, 484–492

The Effect of Transient Eddy on Interannual Meridional Displacement of Summer East Asian Subtropical Jet

XIANG Yang (向 洋) and YANG Xiuqun* (杨修群)

Institute for Climate and Global Change Research, School of Atmospheric Sciences,

Nanjing University, Nanjing 210093

(Received 14 July 2011; revised 8 November 2011)

ABSTRACT

Using ERA-40 reanalysis daily data for the period 1958–2002, this study investigated the effect of transient eddy (TE) on the interannual meridional displacement of summer East Asian subtropical jet (EASJ) by conducting a detailed dynamical diagnosis. The summer EASJ axis features a significant interannual coherent meridional displacement. Associated with such a meridional displacement, the TE vorticity forcing anomalies are characterized by a meridional dipole pattern asymmetric about the climatological EASJ axis. The TE vorticity forcing anomalies yield barotropic zonal wind tendencies with a phase meridionally leading the zonal wind anomalies, suggesting that they act to reinforce further meridional displacement of the EASJ and favor a positive feedback in the TE and time-mean flow interaction. However, The TE thermal forcing anomalies induce baroclinic zonal wind tendencies that reduce the vertical shear of zonal wind and atmospheric baroclinicity and eventually suppress the TE activity, favoring a negative feedback in the TE and time-mean flow interaction. Although the two types of TE forcing tend to have opposite feedback roles, the TE vorticity forcing appears to be dominant in the TE effect on the time-mean flow.

Key words: East Asian subtropical jet, transient eddy vorticity forcing, transient eddy thermal forcing

Citation: Xiang, Y., and X. Q. Yang, 2012: The effect of transient eddy on interannual meridional displacement of summer East Asian subtropical jet. *Adv. Atmos. Sci.*, **29**(3), 484–492, doi: 10.1007/s00376-011-1113-5.

1. Introduction

The East Asian subtropical jet (EASJ) is one of the important atmospheric circulation systems over East Asia (Ren et al., 2010, 2011). The seasonal shift of the EASJ is an indicator of the abrupt seasonal transition of the atmospheric circulation regimes in Asia (Yeh et al., 1959), and such a shift can be associated with the establishment of East Asian summer monsoon as well as the meridional migration of Meiyu/Baiu/Changma (a major rain belt) in East Asia (Tao and Chen, 1987; Yang and Webster, 1990; Ding, 1992; Liang and Wang, 1998; Lau et al., 2000). During the past several decades, many investigators have devoted substantial effort to investigating the location, intensity, structure, and variations of the EASJ as well as its connection to the weather and climate (e.g., Krishnamurti, 1961; Blackmon et al., 1977; Murakami and Unninayar, 1977; Kung and Chan, 1981; Cressman, 1984; Dole and Black, 1990; Kang, 1990; Gao and Tao, 1991; Bell et al., 2000; Lu et al., 2002, 2004; Fyfe and Lorenz, 2005). However, the EASJ variations and their impact on the weather and climate of East Asia have been explored extensively in boreal winter; only several studies so far have involved the change of intensity and shift of the EASJ in boreal summer. The meridional displacement of summer EASJ other than its intensity could be related more intimately to the summer rain belt (Lau et al., 2000; Lu, 2004).

The mechanism responsible for the upper-level jet variability is still under dispute. Atmospheric internal dynamical process associated with transient eddy (TE) activity is believed to play a major role. Some studies have proposed that the interaction of the eddy with the mean flow can reinforce zonal wind anomaly (e.g., Shutts, 1983; Illari, 1984; Robertson and Metz, 1989, 1990; Branstator, 1992, 1995; Yu and Hartmann,

*Corresponding author: YANG Xiuqun, xqyang@nju.edu.cn

1993; Cai and Van den Dool, 1994; Feldstein and Lee, 1996; Lorenz and Hartmann, 2001, 2003). However, other studies argued that the eddy feedback may not be important for the evolution of the zonal wind (Feldstein and Lee, 1996; Lee and Feldstein, 1996) and that the eddy feedback is significant only if the bottom drag is sufficiently strong (Robinson, 1996, 2000; Kravtsov and Robertson, 2002). Notably, most of the previous studies have focused on the interaction between the eddy and zonally-averaged zonal wind, less attention, however, has been paid to the interaction of TE with time-mean flow, while the latter is in favor of examining the local wave-flow interaction.

This study investigated the feature of interannual variations of summer EAJS and the effect of TE feedback. The data and diagnostic method used to depict the meridional displacement of summer EASJ are described in section 2. The major results especially the effects of the TE vorticity and thermal forcing anomalies on the summer EASJ variations are presented in section 3. The final section is devoted to a summary of conclusions.

2. Data and method

The dataset used in this study was obtained from the 40-yr European Centre for Medium-Range Weather Forecasts (ECMWF) reanalysis (ERA-40). The daily data for wind, temperature, geopotential height, and surface pressure fields with a horizontal resolution of $2.5° \times 2.5°$ for 44 summer seasons (June, July and August, JJA) for the period 1958–2002 were extracted from ERA-40.

The conventional method of examining the jet stream variation is to perform empirical orthagonal functions (EOF) with respect to the 200 hPa zonal wind (Lu, 2004; Lin and Lu, 2005; Fyfe and Lorenz, 2005). However, the leading EOFs identified from those analyses may exhibit fluctuations of the jet both in location and in strength and width. In view of this argument, in this study, we defined the jet axis with a line passing through the maximal 200 hPa zonal wind, and then performed EOF analysis with respect to the jet axis anomaly to exclusively identify the EASJ's meridional displacement. Such a displacement is more relevant to rain belt in East Asia (Lau et al., 2000; Lu, 2004).

To examine the TE effect, the TE statistics were computed with daily ERA-40 data. The TE is conventionally defined as the synoptic eddy (Blackmon, 1976; Lau and Holopainen, 1984). However, the TE on various time_scales shorter than one season would dynamically contribute to the seasonal-mean climate anomaly. Therefore, in this study the TE is simply defined as the daily deviation from summer average. This definition allows us to include the TE not only on the synoptic timescale but on the subseasonal timescale.

3. Results

3.1 *Interannual variations of the EASJ*

Figure 1 shows the climatological distribution of zonal wind component at 200 hPa in boreal summer. An elongated belt of stronger westerly runs roughly along 40°N; it contains four maximal cores over the Caspian Sea region, Northwestern China, the midlatitudes of the Northwestern Pacific, and the midlatitude Northwestern Atlantic. The former two cores are relatively larger than the latter two, indicating that the EASJ (denoted by the red line in Fig. 1) is consider-

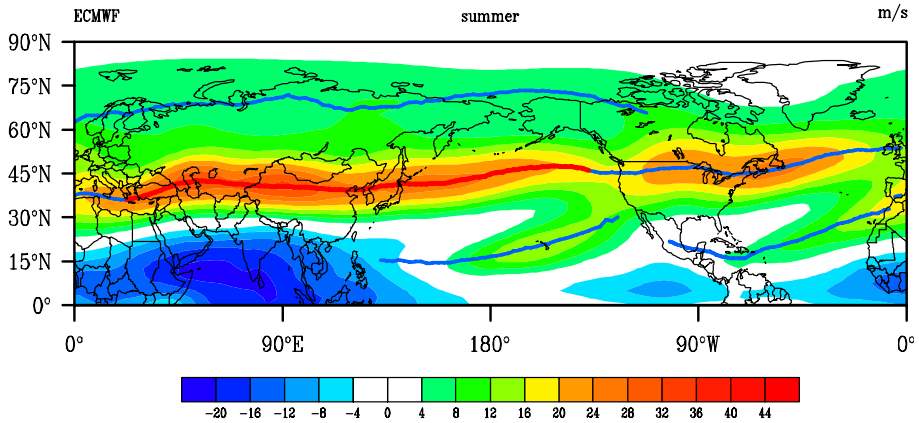

Fig. 1. Climatological 200 hPa zonal wind component in boreal summer (JJA, 1958–2002). The shaded denotes the magnitude of the wind in meters per second (m s^{-1}), and the solid line denotes the axis of the jet stream. The red solid line indicates the axis of the East Asian subtropical jet (EASJ).

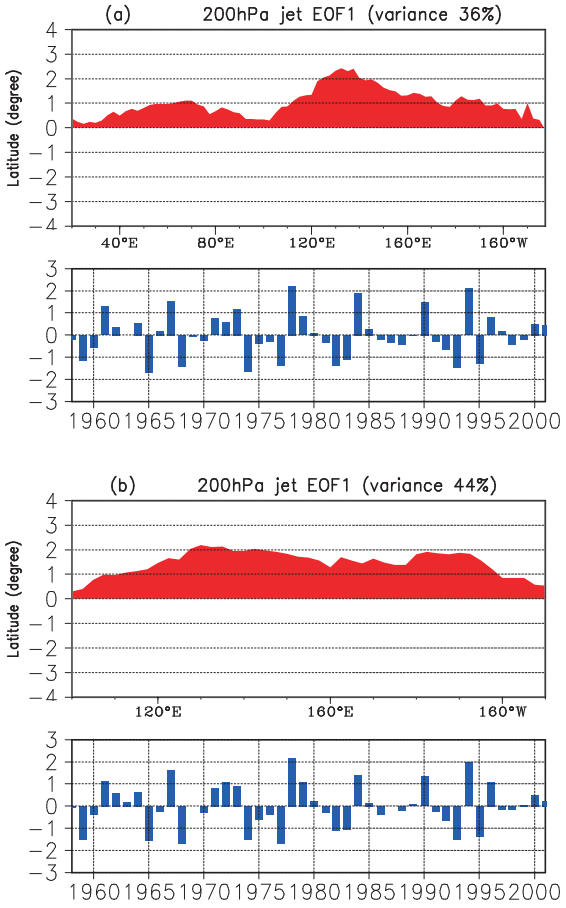

Fig. 2. The leading EOF (upper panel) and the corresponding normalized principal component (bottom panel) of the interannual variations of the summer EASJ axis in latitude at 200 hPa for the domain of (a) 20°E–150°W and (b) 100°E–150°W.

ably stronger than the jet over the mid-latitudes of the Northwestern Atlantic.

The meridional displacement of the EASJ was defined as anomalous deviation from its climatological axis in latitude. A 2–8-year band-pass filter was applied to extract its interannual variations. An EOF analysis on the filtered anomalies of axes in latitude was performed to identify the spatial and temporal distribution of the variation of the EASJ. Figure 2 illustrates the leading EOF of interannual variations of the EASJ axis in boreal summer for different domains. The upper panel of Fig. 2a shows that the EASJ axis is characterized by a significant coherent meridional displacement with up to 2° in latitude, and such a displacement is strikingly larger over the coastal-to-oceanic sector (110°E–160°W) than over the inland sector (20°–110°E). The bottom panel of Fig. 2a displays the corresponding normalized principal component (PC1), indicating that the EASJ axis has a pronounced variation on interannual time_scales. The leading EOF and associated PC1 for the coastal-to-oceanic domain (100°E–150°W) shown in Fig. 2b exhibit spatio-temporal features similar to those shown in Fig. 2a, but they capture more variance.

The atmospheric circulation anomaly pattern associated with the leading EOF of the summer EASJ's interannual variations can be identified by regressing the geopotential height and zonal wind anomalies against the normalized PC1 illustrated in Fig. 2a. Figure 3 shows the latitude-altitude distribution of regressed summer geopotential height and zonal wind anomalies averaged over 110°E–160°W where the EASJ axis has the largest interannual variability. Accompanying the meridional wandering of the EASJ, the geopotential height anomalies with equivalent barotropic structure are located in the vicinity of the climatological EASJ axis. The zonal wind, however, exhibits a meridional dipole pattern asymmetric around the axis. These patterns suggest that a positive geopotential height anomaly near the climatological EASJ axis can result in a westerly acceleration on the poleward side of the climatological EASJ axis and a westerly deceleration

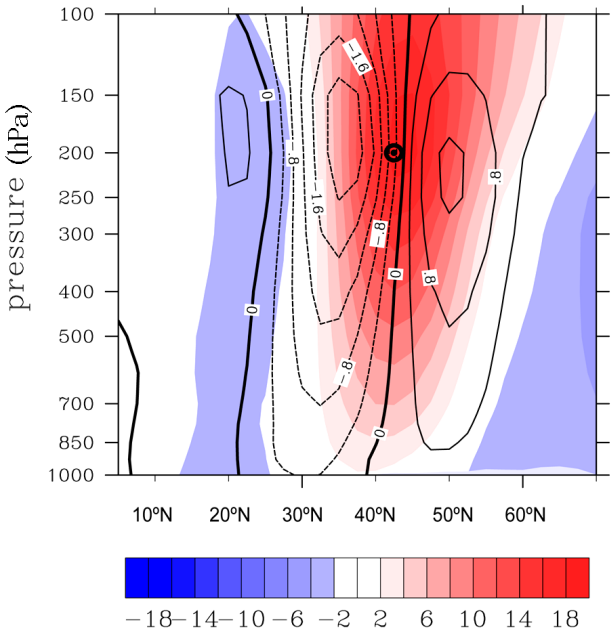

Fig. 3. Latitude-altitude distribution of the summer geopotential height and zonal wind anomalies averaged over 110°E–160°W regressed against the normalized PC1 shown in Fig. 2a. The shaded denotes the geopotential height anomalies in gpm and the contours denote the zonal wind anomalies (units: m s^{-1}). The black circle indicates the climatological location of the summer EASJ axis at 200 hPa.

on the equatorward side, thus leading to a poleward shift of the EASJ and vice versa. Certainly, the geopotential height and zonal wind anomalies satisfy the quasi-geostrophic relation.

3.2 *Associated TE forcing anomalies*

The feedback of TE on time-mean flow is one of fundamental reasons for the time-mean flow anomalies. The TE affects time-mean flow through its vorticity and heat fluxes, which tend to redistribute vorticity and heat in a systematic fashion. The contributions of TE to time-mean flow can be theoretically expressed in terms of the convergences of TE fluxes. Following Pfeffer (1981), Holopainen et al. (1982), and Lau and Holopainen (1984), time-mean quasi-geostrophic potential vorticity (QGPV) equation can be written as

$$\left[\frac{1}{f}\nabla^2 + f\frac{\partial}{\partial p}\left(\frac{1}{\sigma}\frac{\partial}{\partial p}\right)\right]\frac{\partial\overline{\Phi}}{\partial t} = -\nabla\cdot\left(\overline{\boldsymbol{V}'\zeta'}\right) - f\frac{\partial}{\partial p}\left(\frac{R}{\sigma p}Q\right) + R_1, \qquad (1)$$

where the overbar denotes the time average (the summer average here), and the prime the deviation from the time average, Φ is the geopotential, $\boldsymbol{V}$ the horizontal wind vector, and ζ the relative vorticity. R_1 indicates all the remained terms such as horizontal advection, diabatic heating and friction. The left-hand side of Eq. (1) indicates the tendency of time-mean state. The first term of the right-hand side of Eq. (1) is convergence of TE vorticity flux, i.e., the TE vorticity forcing; and the second term is primarily proportional to the vertical gradient of the TE thermal forcing (Q) or the TE heating term, i.e., the convergence of TE heat flux, which is expressed as

$$Q = -\overline{\nabla\cdot\left(\boldsymbol{V}'T'\right)} - \overline{\frac{\partial}{\partial p}\omega'T'} + \overline{\frac{1}{c_p}\frac{RT'}{p}\omega'}, \qquad (2)$$

where ω is the vertical velocity, and T is the temperature.

To estimate the contribution of different timescale TE to the TE forcing, the daily ERA-40 data is bandpass filtered to retain the synoptic (2.5–6 days) and subseasonal ($\sim$ 7–90 days) components, respectively. Thus, the total TE forcing can be separated into two parts: synoptic versus subseasonal components. Figures 4 and 5 show latitude-altitude distributions of the synoptic, subseasonal and total TE vorticity forcing $[-\nabla\cdot(\overline{\boldsymbol{V}'\zeta'})]$ and TE thermal forcing (Q) anomalies, respectively, regressed against the PC1 illustrated in Fig. 2a. It can be seen that both the synoptic TE forcing anomalies and the subseasonal TE forcing anomalies roughly possess structure similar to that of the total TE forcing anomalies. Moreover, the subseasonal TE forcing is comparable to and even larger than the synoptic TE forcing. This suggests that the TE forcing only based on the synoptic time scale is obviously underestimated for the seasonal mean climate anomaly. Therefore, the TE defined in this study as the deviation from summer average can consider not only the synoptic but subseasonal eddy. Dynamically, the TE forcing for either timescale is important and must be considered for determining the seasonal mean climate anomaly, although the synoptic eddy was only addressed in previous studies.

The total TE vorticity forcing anomalies (the TE vorticity forcing anomalies, hereinafter) shown in Fig. 4c are characterized by a meridional dipole pattern asymmetric about the climatological EASJ axis, similar to that of the zonal wind anomalies shown in Fig. 3. As the EASJ displaces northward, the convergent TE vorticity fluxes (i.e., positive TE vorticity forcing) locate to the southern flank of the EASJ, while the divergent TE vorticity fluxes (i.e., negative TE vorticity forcing) locate to its northern flank, and vice versa. However, unlike the distribution of the TE vorticity forcing anomalies, regressed total TE thermal forcing anomalies (the TE thermal forcing anomalies, hereinafter) exhibit a sandwich-like pattern (Fig. 5c). Corresponding to the northward displacement of the EASJ, a considerably large TE cooling (i.e., a divergence of the TE heat fluxes) locates around the climatological EASJ axis and a TE heating (i.e., a convergence of the TE heat fluxes) locates at either side, especially northern side, of the axis.

Notably, there is a difference in vertical structure between the TE vorticity forcing anomalies in Fig. 4c and the zonal wind anomalies in Fig. 3. In Fig. 3, there is a clear vertical tilt for the zonal wind anomalies. Such a tilt is an important feature associated with EASJ meridional displacement. Previous studies suggested that the vertically sheared climatological meridional flow over the western north Pacific may induce the tilt (Kosaka and Nakamura, 2006), or that subtropical precipitation anomalies are responsible for tilt (Lu and Lin, 2009). The present study indicates that the TE may not be responsible for the tilt.

3.3 *The effect of TE forcing anomalies*

The effect of TE on time-mean flow may be approached by treating the convergences of TE fluxes as virtual sources or sinks of heat and vorticity, and solving for the response to these sources or sinks. In this study, we examine initial atmospheric response to the TE forcing anomalies by solving a quasi-geostrophic potential vorticity (QGPV) equation together with appropriate boundary conditions. In terms of Eq. (1),

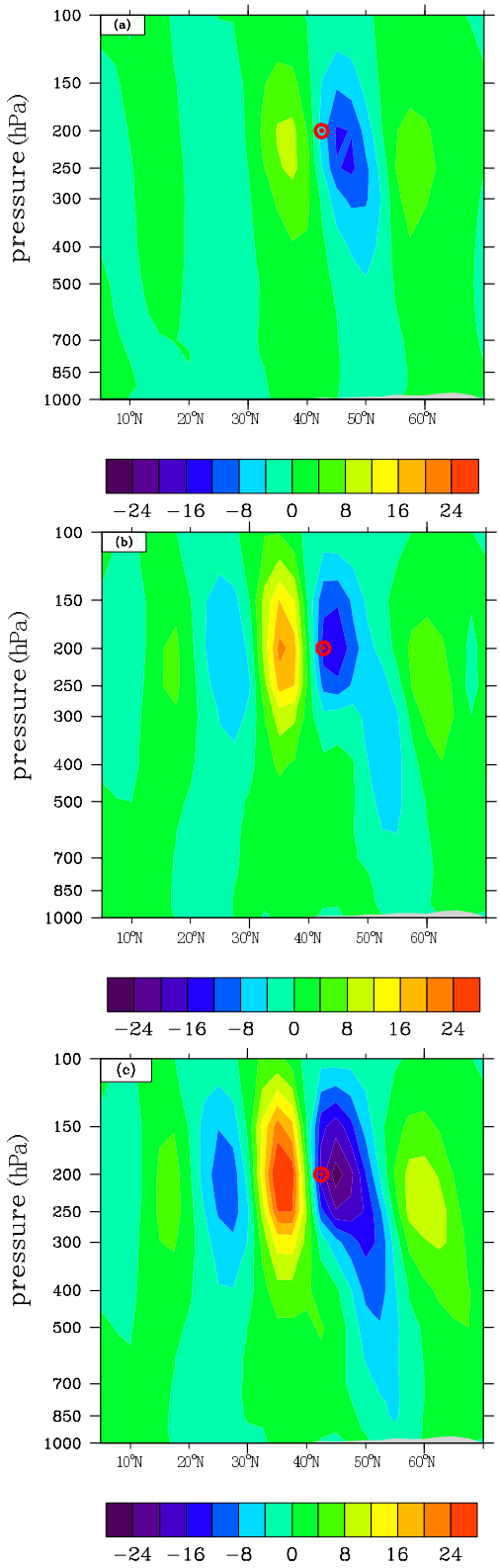

Fig. 4. Same as Fig. 3, but for the (a) synoptic, (b) subseasonal, and (c) total TE vorticity forcing anomalies (10^{-12} s^{-1}). The red circle indicates the climatological location of the summer EASJ axis at 200 hPa.

the initial PV tendency, which is determined by either TE vorticity or thermal forcing anomaly, may be written as

$$\left[\frac{1}{f}\nabla^2 + f\frac{\partial}{\partial p}\left(\frac{1}{\sigma}\frac{\partial}{\partial p}\right)\right]\left(\frac{\partial\overline{\Phi}}{\partial t}\right)_{\text{vort}} = -\nabla\cdot(\overline{\boldsymbol{V}'\zeta'}), \tag{3a}$$

$$\left[\frac{1}{f}\nabla^2 + f\frac{\partial}{\partial p}\left(\frac{1}{\sigma}\frac{\partial}{\partial p}\right)\right]\left(\frac{\partial\overline{\Phi}}{\partial t}\right)_{\text{heat}} = -f\frac{\partial}{\partial p}\left(\frac{R}{\sigma p}Q\right), \tag{3b}$$

where $(\partial\overline{\Phi}/\partial t)_{\text{vort}}$ and $(\partial\overline{\Phi}/\partial t)_{\text{heat}}$ represent the initial tendencies of geopotential due to TE vorticity and thermal forcing, respectively. The solutions to the Eq. (3) were obtained using a method similar to that used by Lau and Holopainen (1984), except that the finite-difference scheme other than spectral truncation scheme was adopted here. The equation was solved for the domain vertically from 1000 hPa to 100 hPa, and meridionally from 0 to 80°N. The vertical and horizontal resolutions used were 50 hPa and 2.5° by 2.5°, respectively. The lateral boundary conditions for the tendency were assumed to be zero. The vertical boundary conditions adopted here were essentially similar to that used in Bretherton (1966) and Lau and Holopainen (1984).

Three-dimensional TE vorticity and thermal forcing anomalies regressed against the PC1 in Fig. 2a, as shown in Figs. 4c and 5c for two dimensions, were applied to the right-hand sides of Eqs. (3a) and (3b), respectively, and then the geopotential tendency together with the geostrophic wind tendency were obtained by solving Eq. (3). Figure 6 shows the latitude–altitude distribution of tendencies of geopotential and zonal wind anomalies induced by regressed TE vorticity forcing anomalies, TE thermal forcing anomalies, and combined TE vorticity and thermal forcing anomalies, respectively. The geopential tendencies induced by TE vorticity forcing anomalies shown in Fig. 6a are characterized by a dipole pattern with distinct equivalent barotropic structure. Consequently, under the geostrophic balance, the zonal wind tendencies exhibit a sandwich-like pattern. These patterns indicate that, in accordance with a positive PC1 illustrated in Fig. 2a (i.e., a northward displacement of the EASJ), there is a significant positive geopotential tendency north of the climatological EASJ axis that produces a negative zonal wind tendency (i.e., decelerating zonal wind) near the climatological axis and a positive zonal wind tendency (i.e., accelerating zonal wind) far north of the axis. A comparison of Fig. 6a and Fig. 3 reveals that the geopotential and zonal wind tendencies induced by the TE vorticity forcing possess a phase that meridionally leads the geopotential height and

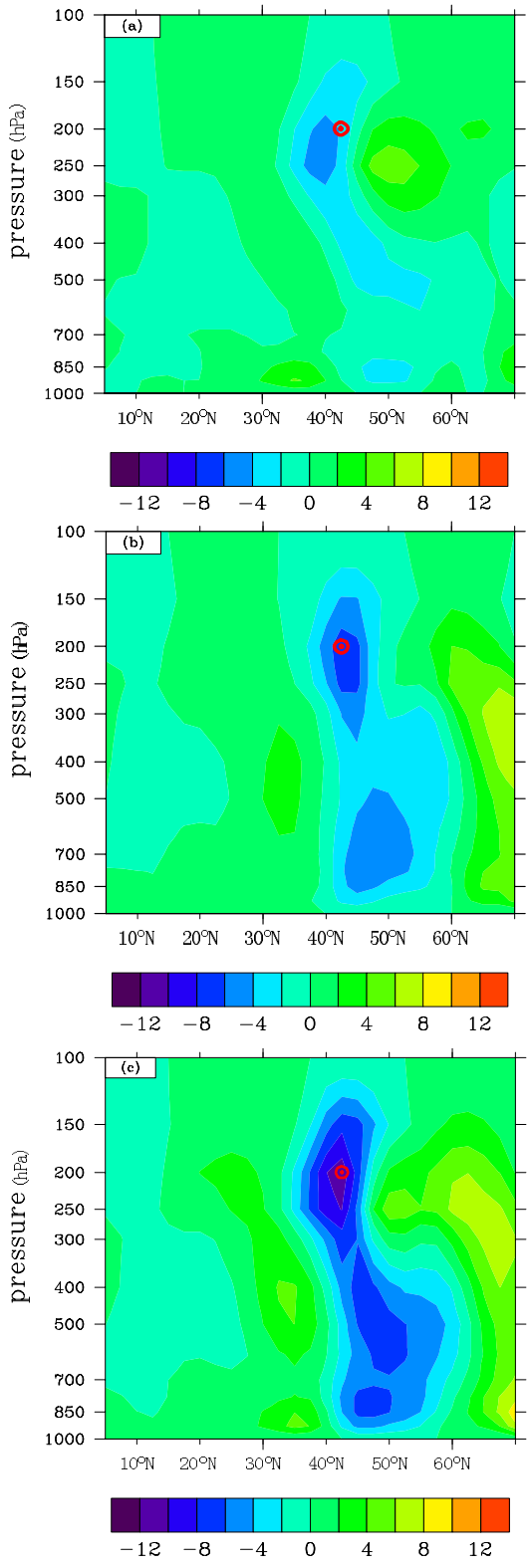

Fig. 5. Same as Fig. 3, but for the (a) synoptic, (b) subseasonal, and (c) total TE thermal forcing anomalies (10^{-7} s^{-1}). The red circle indicates the climatological location of the summer EASJ axis at 200 hPa.

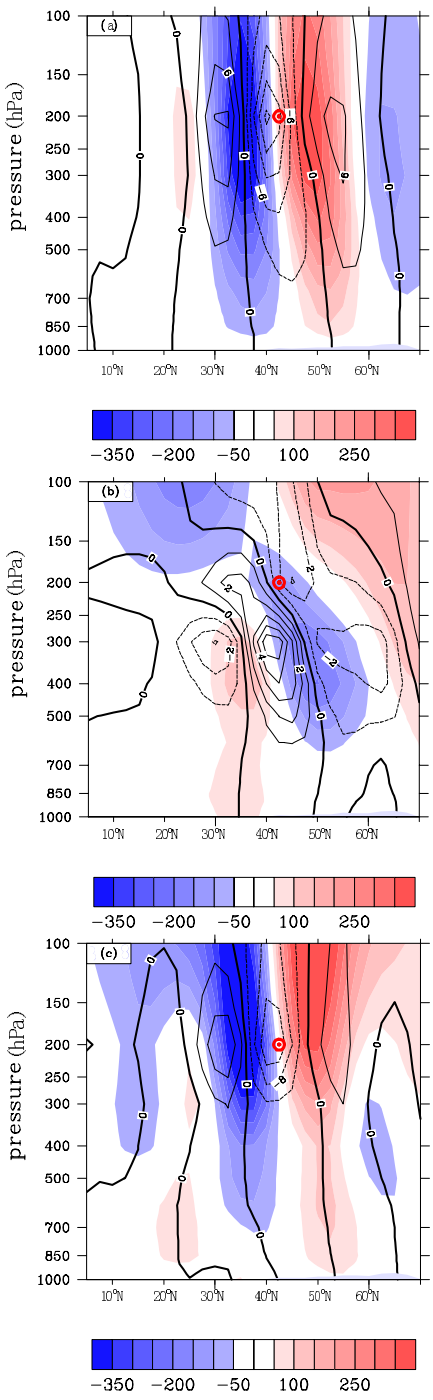

Fig. 6. Latitude-altitude distribution of the tendencies of summer geopotential (shaded, units: m^2 s^{-2} $month^{-1}$) and zonal geostrophic wind (contour, units: m s^{-1} $month^{-1}$) anomalies averaged over 110°E–160°W induced by (a) the regressed TE vorticity forcing anomalies, (b) the regressed TE thermal forcing anomalies, and (c) the combined regressed TE vorticity and thermal forcing anomalies against the normalized PC1 shown in Fig. 2a. The red circle indicates the climatological location of the summer EASJ axis at 200 hPa.

zonal wind anomalies themselves by roughly $\pi/2$. This phase shift suggests that the TE vorticity forcing anomalies act to reinforce further northward progression of the EASJ as it moves northward, and vice versa. Thus, the TE vorticity forcing tends to play a positive feedback role in the interaction between the TE and the time-mean flow.

The TE thermal forcing tends to give rise to a baroclinic response (Fig. 6b). Negative geopotential tendencies occur on the poleward side under the axis of the EASJ, and smaller positive geopotential tendencies occur on the equatorward side beneath the axis of the EASJ. As a result, the zonal geostrophic wind tendencies are characterized by westerly acceleration beneath the axis but deceleration above the axis, especially north of the climatological EASJ axis. This suggests that the TE thermal forcing anomalies act to reduce the vertical shear of zonal wind and thus reduce the atmospheric baroclinicity, which eventually suppresses the TE activity, as the EASJ moves northward. Thus, the TE thermal forcing tends to play a negative feedback role in the interaction between the TE and the time-mean flow.

However, by looking at the Fig. 6c, it can be clearly seen that the combined TE vorticity and thermal forcing anomalies lead to the geopotential and zonal geostrophic wind tendencies similar to those induced by the TE vorticity forcing anomalies only. This indicates that the TE vorticity forcing play a dominant role in the TE effect on the time-mean flow.

4. Summary

Using ERA-40 reanalysis daily data from the period 1958–2002, this study investigated the effect of the TE forcing anomalies on the summer EASJ through a detailed dynamical diagnosis. The TE forcing anomalies were separated into two parts: synoptic versus subseasonal components. The latter may even make a larger contribution to the total TE forcing anomalies. The results demonstrate that the summer EASJ axis features a significant interannual coherent meridional displacement up to 2° in latitude. Associated with this meridional displacement, the TE vorticity forcing anomalies are characterized by a meridional dipole pattern. As the EASJ displaces northward, the convergent TE vorticity fluxes (i.e., positive TE vorticity forcing) occur on the southern flank of the climatological EASJ axis, whereas the divergent TE vorticity fluxes (i.e., negative TE vorticity forcing) occur on its northern flank; as the EASJ displaces southward, the divergent TE vorticity fluxes occur on the southern flank of the climatological EASJ axis, whereas the convergent TE vorticity fluxes occur on its northern flank. However, unlike the distribution of the TE vorticity forcing anomalies, the TE thermal forcing anomalies exhibit a sandwich-like pattern. Corresponding to a northward displacement of the EASJ, a considerably large TE cooling (i.e., a divergence of the TE heat fluxes) occurs around the climatological EASJ axis and a TE heating (i.e., a convergence of the TE heat fluxes) occurs at either side, especially the northern side, of the axis.

The TE vorticity forcing anomalies with a meridional dipole pattern yield barotropic zonal wind tendencies with a phase meridionally leading the zonal wind anomalies by roughly $\pi/2$, suggesting that the TE vorticity forcing anomalies act to reinforce further northward progression of the EASJ as it moves northward. Thus, the TE vorticity forcing tends to play a positive feedback role in the interaction of the TE with the time-mean flow. However, the TE thermal forcing anomalies give rise to baroclinic zonal wind tendencies, which are characterized by westerly acceleration below the axis but deceleration above the axis, especially north of the climatological EASJ axis, as the EASJ moves northward. These tendencies suggest that the TE thermal forcing anomalies act to reduce the vertical shear of zonal wind and thus the atmospheric baroclinicity, which eventually suppresses the TE activity, as the EASJ moves northward. Thus, the TE thermal forcing tends to play a negative feedback role in the interaction of the TE with the time-mean flow. Although the two types of TE forcing tend to have opposite feedback roles, the TE vorticity forcing appears to be dominant in the TE effect on the time-mean flow.

There are some drawbacks that may limit the knowledge gained from this study. For example, we only considered the initial tendency of the time-mean flow as the TE forcing was applied to the QGPV equation. Notably, such a tendency would eventually result in a response with sufficiently large amplitude so that diabatic heating, advection, and friction have to be considered. Moreover, this study aimed to resolve the EASJ variations only from a perspective of internal dynamics, without considering any external forcing. In fact, various external forcing anomalies, such as those in sea surface temperature, thermal condition over Tibetan Plateau, and Euro-Asian snow cover, would greatly affect the EASJ variations. However, these external forcings may exert more influence on the EASJ variations through the TE feedback. A future study is needed to address these combined effects.

Acknowledgements. This work was jointly supported by the National Natural Science Foundation of China (Grant Nos. 40730953 and 40805025), the 973

program (Grant No. 2010CB428504), the National Public Benefit Research Foundation of China (Grant No. GYHY200806004), and the Jiangsu Natural Science Foundation (Grant No. BK2008027). The ERA-40 data were obtained from the ECMWF data server.

REFERENCES

Bell, G. D., and Coauthors, 2000: Climate assessment for 1999. *Bull. Amer. Meteor. Soc.*, **81**, S1–S50.

Blackmon, M. L., 1976: A climatological spectral study of the 500mb geopotential height of the Northern Hemisphere. *J. Atmos. Sci.*, **33**, 1607–1623.

Blackmon, M. L., J. M. Wallace, N. C. Lau, and S. L. Mullen, 1977: An observation study of the Northern Hemisphere wintertime circulation. *J. Atmos. Sci.*, **34**, 1040–1053.

Branstator, G. W., 1992: The maintenance of low-frequency atmospheric anomalies. *J. Atmos. Sci.*, **49**, 1924–1945.

Branstator, G. W., 1995: Organization of storm track anomalies by recurring low-frequency circulation anomalies. *J. Atmos. Sci.*, **52**, 207–226.

Bretherton, F. B., 1966: Critical layers instability in baroclinic flows. *Quart. J. Roy. Meteor. Soc.*, **92**, 325–334.

Cai, M., and H. M. Van den Dool, 1994: Dynamical decomposition of low- and high-frequency tendencies. *J. Atmos. Sci.*, **51**, 2086–2100.

Cressman, G. P., 1984: Energy transformations in the East Asia–West Pacific jet stream. *Mon. Wea. Rev.*, **112**, 563–574.

Ding, Y. H., 1992: Summer monsoon rainfalls in China. *J. Meteor. Soc. Japan*, **70**, 373–396.

Dole, R. M., and R. X. Black, 1990: Life cycles of persistent anomalies. Part II: The development of persistent negative height anomalies over the North Pacific Ocean. *Mon. Wea. Rev.*, **118**, 824–846.

Feldstein, S. B., and S. Lee, 1996: Mechanisms of zonal index variability in an aquaplanet GCM. *J. Atmos. Sci.*, **53**, 3541–3555.

Fyfe, J. C., and D. J. Lorenz, 2005: Characterizing midlatitude jet variability: Lessons from a simple GCM. *J. Climate*, **18**, 3400–3405.

Gao, S., and S. Tao, 1991: Acceleration of upper-tropospheric jet stream and lower-tropospheric frontogenesis. *Chinese J. Atmos. Soc.*, **15**, 11–21.

Holopainen, E. O., L. Rontu, and N. C. Lau, 1982: The effect of large-scale transient eddies on the time–mean flow in the atmosphere. *J. Atmos. Sci.*, **39**, 1971–1984.

Illari, L., 1984: A diagnostic study of the potential vorticity in a warm blocking anticyclone. *J. Atmos. Sci.*, **41**, 3518–3526.

Kang, I. S., 1990: Influence of zonal mean flow change on stationary wave fluctuations. *J. Atmos. Sci.*, **47**, 141–147.

Kosaka, Y., and H. Nakamura, 2006: Structure and dynamics of the summertime Pacific-Japan (PJ) teleconnection pattern. *Quart. J. Roy. Meteor. Soc.*, **132**, 2009–2030.

Kung, E. C., and P. H. Chan, 1981: Energetics characteristics of the Asian winter monsoon in the source region. *Mon. Wea. Rev.*, **109**, 854–870.

Kravtsov, S., and A. W. Robertson, 2002: Midlatitude ocean–atmosphere interaction in an idealized coupled model. *Climate Dyn.*, **19**, 693–711.

Krishnamurti, T. N., 1961: The subtropical jet stream of winter. *J. Meteor.*, **18**, 172–191.

Lau, K. M., K. M. Kim, and S. Yang, 2000: Dynamical and boundary forcing characteristics of regional components of the Asian summer monsoon. *J. Climate*, **13**, 2461–2482.

Lau, N. C., and E. O. Holopainen, 1984: Transient eddy forcing of the time–mean flow as identified by geopotential tendencies. *J. Atmos. Sci.*, **41**, 313–328.

Lee, S., and S. B. Feldstein, 1996: Mechanisms of zonal index evolution in a two-layer model. *J. Atmos. Sci.*, **53**, 2232–2246.

Liang, X. Z., and W. C. Wang, 1998: Associations between China monsoon rainfall and tropospheric jets. *Quart. J. Roy. Meteor. Soc.*, **124**, 2597–2623.

Lorenz, D. J., and D. L. Hartmann, 2001: Eddy–zonal flow feedback in the Southern Hemisphere. *J. Atmos. Sci.*, **58**, 3312–3327.

Lorenz, D. J., and D. L. Hartmann, 2003: Eddy–zonal flow feedback in the Northern Hemisphere winter. *J. Climate*, **16**, 1212–1227.

Lu, R., J. H. Oh, B. J. Kim, 2002: A teleconnection pattern in the upper-level meridional wind over the North African and Eurasian continent in summer. *Tellus*, **54A**, 44–55.

Lu, R., 2004: Associations among the components of the East Asian summer monsoon systems in the meridional direction. *J. Meteor. Soc. Japan*, **82**, 155–165.

Lu, R., and Z. Lin, 2009: Role of subtropical precipitation anomalies in maintaining the summertime meridional teleconnection over the western North Pacific and East Asia. *J. Climate*, **22**, 2058–2072.

Lin, Z., and R. Lu, 2005: Interannual meridional displacement of the East Asian upper-tropospheric jet stream in summer. *Adv. Atmos. Sci.*, **22** , 199–211.

Murakami, T., and M. Unninayar, 1977: Atmospheric circulation during December 1970 through February 1971. *Mon. Wea. Rev.*, **105**, 1024–1038.

Pfeffer, R. L., 1981: Wave-mean flow interactions in the atmosphere. *J. Atmos. Sci.*, **38**, 734–744.

Ren, X., X. Yang, and C. Chu, 2010: Seasonal variations of the synoptic-scale transient eddy activity and polar–front jet over East Asia. *J. Climate*, **23**, 3222–3233.

Ren, X., X. Yang, T. Zhou, and J. Fang, 2011: Diagnostic comparison of wintertime East Asian subtropical jet and polar-front jet: Large–scale characteristics and transient eddy activities. *Acta Meteorologica Sinica*, **25**, 21–33.

Robertson, A. W., and W. Metz, 1989: Three-

dimensional instability of persistent anomalous large-scale flows. *J. Atmos. Sci.*, **46**, 2783–2801.

Robertson, A. W., and W. Metz, 1990: Transient eddy feedbacks derived from linear theory and observations. *J. Atmos. Sci.*, **47**, 2743–2764.

Robinson, W., 1996: Does eddy feedback sustain variability in the zonal index? *J. Atmos. Sci.*, **53**, 3556–3569.

Robinson, W., 2000: A baroclinic mechanism for the eddy feedback on the zonal index. *J. Atmos. Sci.*, **57**, 415–422.

Shutts, G. J., 1983: The propagation of eddies in diffluent jet streams: Eddy vorticity forcing of blocking flow fields. *Quart. J. Roy. Meteor. Soc.*, **109**, 737–761.

Tao, S. Y., and L. X. Chen, 1987: A review of recent research of the East Asian summer monsoon in China. *Monsoon Meteorology*, Chang and Krishnamurti, Eds., Oxford University Press, 60–92.

Yang, S., and P. J. Webster, 1990: The effect of summer tropical heating on the location and intensity of the extratropical westerly jet streams. *J. Geophys. Res.*, **95**, 18705–18721.

Yeh, T. C., S. Y. Tao, and M. T. Li, 1959: The abrupt change of circulation over the Northern Hemisphere during June and October. *The Atmosphere and the Sea in Motion*, B. Bolin, Ed., Rockefeller Institute Press, 249–267.

Yu, J. Y., and D. L. Hartmann, 1993: Zonal flow vacillation and eddy forcing in a simple GCM of the atmosphere. *J. Atmos. Sci.*, **50**, 3244–3259.